CLAY MINERALS AS HOST MATRICES FOR DIFFERENT ANTIMICROBIAL AGENTS: THEORETICAL STUDY

HLAVÁČ Dominik [1]

[1] *VŠB - TECHNICAL UNIVERSITY OF OSTRAVA, 17. listopadu 15, 708 33 Ostrava - Poruba, Czech Republic, dominik.hlavac@vsb.cz.*

Abstract

This work is focused on exploration of capability of zero charged clay minerals kaolinite and pyrophyllite to carry antibacterial chlorhexidine and antifungal nystatin, respectively. Investigation of host-guest interaction was based on force field molecular dynamics which was performed on model surfaces in periodic boundary conditions. Comparison of mean binding energies was used in selection of appropriate matrix and improvement of antibacterial activity was estimated on the basis of available experimental data. Further investigation included calculation of mean square displacements of antimicrobial agents in order to estimate their diffusion over the surface and thus make an estimation of adsorption rate. Finally, differences of guest's shape were observed on the basis of structural characteristic - radius of gyration.

Keywords:

molecular dynamics, chlorhexidine, nystatin, kaolinite, pyrophyllite

1. INTRODUCTION

Growing demand of more effective antimicrobial agents is observed in many areas involving food processing and packaging [1], water cleaning [2], hygiene or medicine [3,4]. Chlorhexidine (CH) having two ionizable guanidine moieties is the most widely used biocide in antiseptic products, dental medicine [5] and orthopedics [6]. Although usage of CH in everyday praxis is considered to be safe, the toxicity at a certain level of concentration was reported [7]. Therefore, better utilization may be achieved by incorporation of CH into appropriate matrix. In certain cases also other microbes except bacteria have to be eliminated and Nystatin (Nys) showing excellent behavior against fungal *Candida* strains [8,9] represents effective compound in treatment of cutaneous and mucocutaneous fungal infections [10]. In order to enhance Nys utilization and suppress its poor water solubility, several delivery systems were proposed [10–14]. Despite wide usage of Nys in clinical praxis [15], acute generalized exanthematous pustulosis was reported [16]. Therefore, development of optimal delivery systems is still very relevant topic.

Usage of both antibacterial CH and antifungal Nys agents has its limitations and difficulties. In order to overcome them, incorporation into suitable matrices seems to be promising way. Natural clays are reasonable choice for further investigation due to their high surface area, wide availability, low cost and zero toxicity. Although several experimental and theoretical studies focused on preparation and/or characterization of CH/clays nanocomposites exist [17-21], there is a lack of any systematic classification of clay's docking capabilities for CH. In addition, to the best knowledge, no clay-based composite material containing Nys was reported hitherto. Docking capabilities of clay minerals differ from each other (in dependence on the surface area, the host-guest interaction and the method of preparation) and the selection of the best ones according to the knowledge of host-guest interaction is necessary. This information can be obtained using molecular modeling. The aim of this work is to explore the capability of zero-charged clay minerals kaolinite (KLT) and pyrophyllite (PYR) to carry antibacterial CH and antifungal Nys, respectively. Comparison of both matrices was done with respect to the values of calculated binding energies (E_{bind}), mean square displacement (MSD) of active agents, and radii of gyration (RoG).

2. SIMULATION DETAILS

2.1 Model structures

Antimicrobial agents CH and Nys were sketched in Materials Studio 4.2 (MS) module Visualizer. CH was simulated as 2+ cation, hydrogen atoms were located at "backbone" nitrogens as in [22]. Models of clays were prepared according to available crystallochemical data (KLT [23], PYR [24]) as 5*a* × 3*b* × 1*c* supercells. Since poor intercalation of KLT and PYR by larger organic compounds is well known, only models of surfaces were prepared. The models consisted of two clay layers separated by 5 nm vacuum slab and one CH or Nys molecule. Presence of other molecules was not considered (i.e. further CH and/or Nys molecules, water, etc.). It should be mentioned that in the case of KLT two kinds of surfaces are exposed to adsorbates and, therefore, both octahedral (KLT_O) as well as tetrahedral (KLT_T) were investigated.

2.2 Simulation parameters

Discover module of MS was used in this study. After preliminary energy minimization, 1 ns long trajectory was recorded. Canonical ensemble NVT was established for the simulation and temperature was adjusted by direct velocity scaling. Integration of equations of motion was performed using velocity Verlet algorithm. Potential energy parameters of interCVFF force-field from Heinz et al. [25] were used in simulation, because they showed excellent agreement between calculated and experimental values of surface related properties (cleavage energy/surface energy) [26], thus ensuring their applicability for considered model systems. Models of surfaces were calculated under periodic boundary conditions.

2.3 Calculated properties

Adhesion of atoms or molecules on surfaces is often estimated on the basis of binding energies. These are usually calculated using eq. 1,

$$E_{bind} = E_{sys} - E_{mol} - E_{clay} \qquad \text{eq. 1}$$

where the binding energy E_{bind} is defined as the difference between the potential energy of the whole simulated system E_{sys}, the energy of adsorbed molecule E_{mol} and the energy of host surface E_{clay}. Except differences in thermodynamical costs accompanied with adsorption/desorption of molecules (expressed in terms of E_{bind}), also nuances in their structure and mobility on KLT and PYR were recorded. Mobility of molecules was observed using the mean square displacement (MSD) of their centre of mass (CoM) calculated as in eq. 2,

$$MSD(n) = \frac{1}{N-n}\sum_{i=1}^{N-n}\left|\vec{r}_{i+n} - \vec{r}_i\right|^2, \qquad n = 1,....,N-1 \qquad \text{eq. 2}$$

where n represents distinct time interval in which position vectors of CoM are recorded, and N represents total time of simulation. Knowledge of MSD further enables calculation of molecule's diffusion coefficient D through the Einstein relation (eq. 3). Because our study is limited to study of adsorbed molecules, only movement perpendicular to the norm of surface was considered and, therefore, number of degrees of freedom n_{DF} equals 2.

$$MSD(n) = n_{DF} \cdot 2 \cdot D \cdot t_n \qquad \text{eq. 3}$$

Plotting calculated values of MSD in dependence on time t_n which corresponds to appropriate time intervals n should yield straight line and value D can be deduced from the slope of the curve.

Structural changes of adhered molecules were characterized by radius of gyration (RoG). This structural property describes shape of the molecule through the information about distribution of mass around CoM.

Square of RoG is defined as squared distance of each molecule's atom from the CoM (eq. 4) weighted by atom's mass m_j and divided by the total mass of molecule (M is total number of atoms forming the molecule).

$$RoG^2 = \frac{\sum_j^M m_j \left|\vec{r}_j - \vec{r}_{CoM}\right|^2}{\sum_j^M m_j} \qquad \text{eq. 4}$$

3. RESULTS AND DISCUSSION

3.1 Binding energies

Calculated binding energies are listed in Table 1. Although CH and Nys exhibit quite similar properties (both are constituted from polar as well as non-polar parts and are miscible with similar solvents), their adsorption to clay matrices is driven by different forces. While in the case of KLT (both KLT_O and KLT_T) the E_{bind} of Nys is weaker than that of CH, this completely turns over when PYR is chosen as the host matrix. Another clue indicating different adsorption is different preference of KLT_O surface by Nys and CH. While KLT_T is rather preferred by CH (Table 1 and [21]), stronger adsorption on KLT_O was found in case of Nys. This is probably related to higher number of hydrogen bond forming constituents (HBC) on Nys. Although direct mechanism of adsorption remains unclear, several predictions can be already stated. First of all, enhancement of antibacterial effect of CH reported in [20] may be expected if PYR will be used as the host matrix. On the contrary, lower content of Nys than that of CH will be probably adsorbed on KLT. Finally, taking into account that much greater E_{bind} value is achieved when PYR serves as the host matrix, utilization of PYR rather than KLT in Nys adsorption is proposed.

Table 1 Binding energies (E_{bind}) and coefficients of lateral diffusion (D) of CH and Nys molecules on different surfaces. Standard deviations of presented mean values are introduced in the brackets.

	E_{bind} (mJ/m^2)				D (m^2/s)	
surface	CH		Nys		CH	Nys
KLT_O	-78.53	(5.19)	-38.90	(4.46)	$1.25 \cdot 10^{-9}$	$2.54 \cdot 10^{-9}$
KLT_T	-82.67	(2.94)	-35.15	(3.05)	$2.97 \cdot 10^{-9}$	$4.17 \cdot 10^{-9}$
PYR	-277.57	(4.58)	-467.51	(3.59)	$1.39 \cdot 10^{-7}$	$5.03 \cdot 10^{-9}$

3.2 Surface mobility

In order to estimate the rate of adsorption, MSD of individual CH and Nys agents was measured (Fig. 1) and corresponding D was calculated (Table 1). It is apparent that while MSD of Nys on PYR and KLT_T is similar and only slightly different from Nys on KLT_O (Fig. 1b), in case of CH the situation is different (Fig. 1a). CH exhibits substantial difference between mobility on KLT_T, KLT_O and PYR (Fig. 1a). The biggest slope of MSD observed for PYR is much higher than that of KLT_T. On the contrary, difference between mobility of CH on KLT_T and KLT_O (inset in Fig. 1a) is greater than difference between the same matrices in the case of Nys (Fig. 1b). This suggests again that adsorption mechanism of CH and Nys is different. Lowest mobility of both agents on KLT_O corresponds well with higher number of HBC on this matrix. Taking into account higher number of HBC on Nys, one can also interpret smaller differences between mobility on PYR, KLT_T and KLT_O than in the case of CH. Because of higher amount of HBC which are located close to each other, Nys extents over larger area and, therefore, can more easily interact with octahedral hydroxyls hidden in ditrigonal cavities. In this manner it is stabilized through hydrogen bonds and its mobility is decreased. On

the contrary, the same location of HBC can act as “series of wheels” enabling thus rolling over KLT_O. Based on these observations, number and location of HBC seems to be a key factor influencing the rate of adsorption because of relation between lateral diffusion and adsorption of further molecules [27]. In addition, much faster adsorption of CH can be expected on PYR than on KLT.

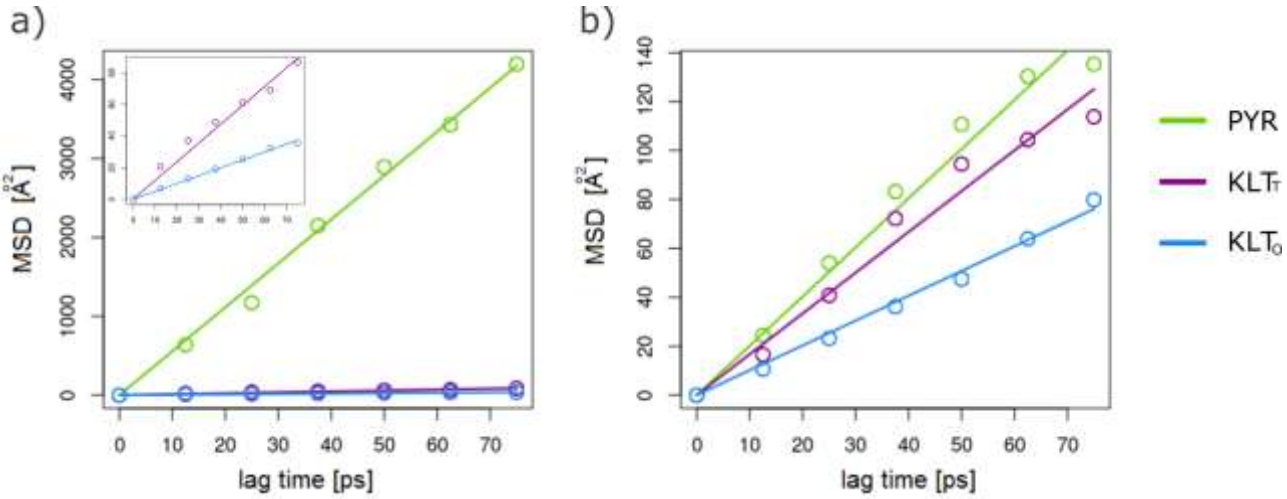

Fig. 1 MSD of (a) CH (b) Nys molecules on different clay matrices. Lines are linear fits to the data points.

3.3 Variations in shape

Changes in shape of CH and Nys are shown in Fig. 2 where the RoG values for adsorbed molecules and for molecules in gas phase (GP) are compared. Behavior of CH and Nys is again different depending on the matrix. Adsorption of Nys and CH on PYR led to more compact shape (i.e. all atoms in molecule are distributed closer around CoM) than adsorption of both agents on KLT. RoG values of CH and Nys adsorbed on PYR are also lower than RoG values for CH and Nys in GP. On the contrary, for Nys adsorbed on KLT_O or KLT_T and for CH adsorbed to KLT_T the RoG values are higher than for CH and Nys in GP. Only CH adsorbed on KLT_O adopted conformations similar to CH in GP. However, their heterogeneity was, like in all other adsorbed states, strongly reduced. The biggest variability of RoG was observed for CH adsorbed to KLT_T, where alternation between more compact assembly and more stretched shape of CH indicates greater mobility of molecule. Stronger interaction between studied agents and PYR than in the case of KLT_O and KLT_T seems to be a consequence of more interacting partners on PYR (added tetrahedral layer). This manifests in adoption of more compact shape of both agents on PYR matrix.

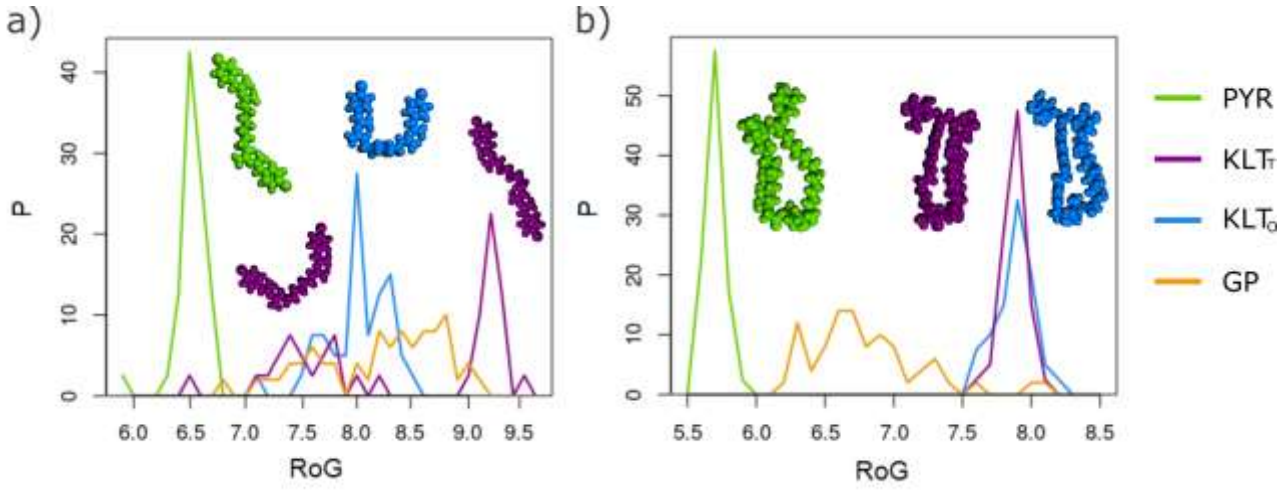

Fig. 2 RoG and top view of (a) CH and (b) Nys molecules on different clay matrices. Corresponding RoG in GP is introduced for comparison.

4. CONCLUSIONS

Comparison of two clay silicates PYR and KLT in terms of their ability to host antimicrobial agents Nys and CH was performed on the basis of molecular dynamics calculations. Calculations of E_{bind} suggest the possibility to improve the antibacterial effect of CH-based nanocomposites by using PYR silicate instead of KLT as the host matrix. Similarly, PYR was selected as the more appropriate matrix for Nys because of stronger mutual interaction. MSD was used to evaluate mobility of CH and Nys over the surfaces and thus estimate the adsorption rate. While in the case of CH much faster adsorption rate is expected on PYR than on KLT, MSD curves of Nys are similar for all investigated surfaces. Differences in shape of investigated molecules adsorbed on PYR and KLT and in GP were investigated using RoG. Greater change in shape dependent on used matrix is exhibited by Nys, although adsorption of both antimicrobial agents leads to reduction of their conformational heterogeneity and adoption of different shape in comparison with GP. While adsorption on PYR leads to conformations where atoms are distributed closer around the CoM, adsorption on KLT results in such shapes that some atoms are more remote from CoM.

ACKNOWLEDGEMENTS

This work was supported by the IT4Innovations Centre of Excellence project (CZ.1.05/1.1.00/02.0070), funded by the European Regional Development Fund and the national budget of the Czech Republic via the Research and Development for Innovations Operational Programme, as well as Czech Ministry of Education, Youth and Sports via the projects Large Research, Development and Innovations Infrastructures (LM2011033) and (SP2015/59).

REFERENCES

[1] SUNG, S.-Y., SIN, L. T., TEE, T.-T. BEE, S.-T., RAHMAT, A. R., RAHMAN, W. A., TAN, A.-C., VIKHRAMAN, M. Antimicrobial agents for food packaging applications. Trends in Food Science and Technology, Vol. 33, No. 2, 2013, pp. 110-123.

[2] HOSSAIN, F. PERALES-PEREZ, O. J., HWANG, S., ROMÁN, F. Antimicrobial nanomaterials as water disinfectant: applications, limitations and future perspectives. The Science of The Total Environment, Vol. 466-467, No. 1, 2014, pp. 1047-1059.

[3] RAHAMAN, M., FURKANUR, M., JAHID, I. K., HA, S.-D. Microbial biofilms in seafood: a food-hygiene challenge. Food Microbiology, Vol. 49, No. 1, 2015, pp. 41-55.

[4] WENDLANDT, S., SHEN, J., KADLEC, K., WANG, Y., LI, B., ZHANG, W.-J., FESSLER, A. T., WU, C., SCHWARZ, S. Multidrug resistance genes in staphylococci from animals that confer resistance to critically and highly important antimicrobial agents in human medicine. Trends in Microbiology, Vol. 23, No. 1, 2015, pp. 44-54.

[5] McDONNELL, G., RUSSELL, A. D. Antiseptics and disinfectants: activity, action, and resistance. Clinical Microbiology Reviews, Vol. 12, No. 1, 1999, pp. 147-179.

[6] SIMCHI, A., TAMJID, E., PISHBIN, F., BOCCACCINI, A. R. Recent progress in inorganic and composite coatings with bactericidal capability for orthopaedic applications. Nanomedicine: Nanotechnology, Biology, and Medicine, Vol. 7, No. 1, 2011, pp. 22-39.

[7] GIANELLI, M., CHELLINI, F., MARGHERI, M., TONELLI, P., TANI, A. Effect of chlorhexidine digluconate on different cell types: A molecular and ultrastructural investigation. Toxicology in Vitro, Vol. 22, No. 2, 2008, pp. 308-317.

[8] RÉCAMIER, K. S., HERNÁNDEZ-GÓMEZ, A., GONZÁLEZ-DAMIÁN, J., ORTEGA-BLAKE, I. Effect of membrane structure on the action of polyenes: I. Nystatin action in cholesterol- and ergosterol-containing membranes. The Journal of Membrane Biology, Vol. 237, No. 1, 2010, pp. 31-40.

[9] SEMIS, R., POLACHECK, I., SEGAL, E. Nystatin-intralipid preparation: characterization and in vitro activity against yeasts and molds. Mycopathologia, Vol. 169, No. 5, 2010, pp. 333-341.

[10] MARTÍN, M. J., CALPENA, A. C., FERNÁNDEZ, F., MALLANDRICH, M., GÁLVEZ, P., CLARES, B. Development of alginate microspheres as nystatin carriers for oral mucosa drug delivery. Carbohydrate Polymers, Vol. 117, No. 1, 2015, pp. 140-149.

[11] BÍLKOVÁ, E., IMRAMOVSKÝ, A., BUCHTA, V., SEDLÁK, M. Targeted antifungal delivery system: beta-glucosidase sensitive nystatin-star poly(ethylene glycol) conjugate. International Journal of Pharmaceutics, Vol. 386, No. 1-2, 2010, pp. 1-5.

[12] PÁL, S., NAGY, S., BOZÓ, T., KOCSIS, B., DÉVAY, A. Technological and biopharmaceutical optimization of nystatin release from a multiparticulate based bioadhesive drug delivery system. European Journal of Pharmaceutical Sciences, Vol. 49, No. 2, 2013, pp. 258-264.

[13] ROSATO, A., VITALI, C., PIARULLI, M., MAZZOTTA, M., ARGENTIERI, M. P., MALLAMACI, R. In vitro synergic efficacy of the combination of Nystatin with the essential oils of Origanum vulgare and Pelargonium graveolens against some Candida species. Phytomedicine: International Journal of Phytotherapy and Phytopharmacology, Vol. 16, No. 10, 2009, pp. 972-975.

[14] RACLES, C., MARES, M., SACARESCU, L. A polysiloxane surfactant dissolves a poorly soluble drug (nystatin) in water. Colloids and Surfaces A: Physicochemical and Engineering Aspects, Vol. 443, No. 1, 2014, pp. 233-239.

[15] MAYS, J. W., SARMADI, M., MOUTSOPOULOS, N. M. Oral manifestations of systemic autoimmune and inflammatory diseases: diagnosis and clinical management. The Journal of Evidence-Based Dental Practice, Vol. 12, No. 3, 2012, pp. 265-282.

[16] OCERIN-GUERRA, I., GOMEZ-BRINGAS, C., ASPE-UNANUE, L., RATÓN-NIETO, J. A. Nystatin-induced acute generalized exanthematous pustulosis. Actas Dermo-Sifiliográficas, Vol. 103, No. 10, 2012, pp. 927-928.

[17] HOLEŠOVÁ, S., VALÁŠKOVÁ, M., PLEVOVÁ, E., PAZDZIORA, E., MATĚJOVÁ, K. Preparation of novel organovermiculites with antibacterial activity using chlorhexidine diacetate. Journal of Colloid and Interface Science, Vol. 342, No. 2, 2010, pp. 593-597.

[18] HLAVÁČ, D., TOKARSKÝ, J. Molecular modeling of vermiculite/chlorhexidine diacetate nanocomposite. Journal of Nanocomposites and Nanoceramics, Vol. 3, No. 1, 2012, pp. 15-19.

[19] HE, H., YANG, D., YUAN, P., SHEN, W., FROST, R. L. A novel organoclay with antibacterial activity prepared from montmorillonite and Chlorhexidini Acetas. Journal of Colloid and Interface Science, Vol. 297, No. 1, 2006, pp. 235-243.

[20] HOLEŠOVÁ, S., VALÁŠKOVÁ, M., HLAVÁČ, D., MADEJOVÁ, J., SAMLÍKOVÁ, M., TOKARSKÝ, J., PAZDZIORA, E. Antibacterial kaolinite/urea/chlorhexidine nanocomposites: Experiment and molecular modelling. Applied Surface Science, Vol. 305, No. 1, 2014, pp. 783-791.

[21] HLAVÁČ, D., TOKARSKÝ, J. Non-Bond Interactions Between Chlorhexidine Diacetate and Kaolinite: a Molecular Modeling Study. In NANOCON 2014: 6th International Conference. Brno: TANGER, 2014, pp. 644-650.

[22] VAN OOSTEN, B., MARQUARDT, D., KOMLJENOVIĆ, I., BRADSHAW, J. P., STERNIN, E., HARROUN, T. A. Small molecule interaction with lipid bilayers: a molecular dynamics study of chlorhexidine. Journal of Molecular Graphics and Modelling, Vol. 48, No. 1, 2014, pp. 96-104.

[23] BISH, D. L. Rietveld refinement of the kaolinite structure at 1.5 K. Clays and Clay Minerals, Vol. 41, No. 6, 1993, pp. 738-744.

[24] LEE, J. H., GUGGENHEIM, S. Single crystal X-ray refinement of pyrophyllite-1*Tc*. American Mineralogist, Vol. 66, No. 3-4, 1981, pp. 350-357.

[25] HEINZ, H., KOERNER, H., ANDERSON, K. L., VAIA, R. A., FARMER, B. L. Force Field for Mica-Type Silicates and Dynamics of Octadecylammonium Chains Grafted to Montmorillonite. Chemistry of Materials, Vol. 17, No. 23, 2005, pp. 5658-5669.

[26] HEINZ, H., LIN, T.-J., KISHORE MISHRA, R., EMAMI, F. S. Thermodynamically Consistent Force Fields for the Assembly of Inorganic, Organic, and Biological Nanostructures: The INTERFACE Force Field. Langmuir, Vol. 29, No. 6, 2013, pp. 1754-1765.

[27] RAVICHANDRAN, S., TALBOT, J. Mobility of adsorbed proteins: a Brownian dynamics study. Biophysical Journal, Vol. 78, No. 1, 2000, pp. 110-120.